Available online at www.sciencedirect.com
ScienceDirect
Applied Surface Science 253 (2006) 1010–1014
applied surface science
www.elsevier.com/locate/apsusc

Quantitative depth profiling of photoacid generators in photoresist materials by near-edge X-ray absorption fine structure spectroscopy☆

Vivek M. Prabhu [a,*], Sharadha Sambasivan [a], Daniel Fischer [b], Linda K. Sundberg [c], Robert D. Allen [c]

[a] *Polymers Division, National Institute of Standards and Technology, Gaithersburg, MD 20899, United States*
[b] *Ceramics Division, National Institute of Standards and Technology, Gaithersburg, MD 20899, United States*
[c] *IBM Almaden Research Center, 650 Harry Road, San Jose, CA 951205, United States*

Received 5 January 2006; accepted 26 March 2006
Available online 9 May 2006

Abstract

Near-edge X-ray absorption fine structure (NEXAFS) spectroscopy was used to quantify the surface composition and depth profiling of photoacid generators in thin film photoresist materials by varying the entrance-grid bias of a partial electron yield detector. By considering model compositional profiles, NEXAFS distinguishes the surface molar excess within the top 6 nm from the bulk. A surface enriched system, triphenylsulfonium perfluorooctanesulfonate, is contrasted with a perfluorobutanesulfonate photoacid generator, which displays an appreciable surface profile within a 6 nm segregation length scale. These results, while applied to 193-nm photoresist materials, highlight a general approach to quantify NEXAFS partial electron yield data.
© 2006 Elsevier B.V. All rights reserved.

Keywords: Immerison lithography; Lithography; Photoresist; Segregation; Near edge X-ray absorption fine spectroscopy; NEXAFS; Thin film

1. Introduction

Chemically amplified photoresists are multi-component systems comprised primarily of polymeric photoresist, photoacid generators (PAGs) and base additives. The distribution of these components within the thin film state is critical to print nanoscale features by photolithography. Near-edge X-ray absorption fine structure (NEXAFS) spectroscopy provides a sensitive bond-selective and depth-selective method to quantify the thin film surface structure [1]. This unique ability is ideally suited to address emerging problems in immersion lithography which uses a fluid, such as water, in contact with the lens system and thin film. Any change in surface structure or chemistry from the top few nanometers due to leaching of PAGs and base additives during immersion can compromise the performance of the resist as well as contaminate the lens system [2,3]. Methods have been developed to quantify the absolute amounts of PAG extracted [4–6], however, discriminating the surface profile remains to be understood within the top 10 nm.

Photoresist thin films exhibit surface segregation of PAGs that is a function of the balance between PAG and resist chemistry. Rutherford backscattering spectroscopy (RBS) was used to understand the miscibility of arsenic and sulfur containing PAGs as a function of photoresist chemistry [7]. Sundararajan et al. used RBS to examine the diffusion and distribution characteristics of PAGs by examining heavy atoms [8]. Krautter et al. studied the surface composition of a variety of PAGs with X-ray photoelectron spectroscopy [9]. They observed the enrichment of perfluorooctanesulfonate in the top few Angstroms from the fluorine atomic composition. However, the top 10 nm was not well characterized due to experimental limitations. We present a methodology to quantify the PAGs depth profile over the top 2–6 nm by NEXAFS spectroscopy which can be extended to a diverse set of resist systems without the need for special labeling or preparatory procedures.

☆ Official contribution of the National Institute of Standards and Technology; not subject to copyright in the United States.

* Corresponding author. Tel.: +1 301 975 3657; fax: +1 301 975 3928.
E-mail address: vprabhu@nist.gov (V.M. Prabhu).

0169-4332/$ – see front matter © 2006 Elsevier B.V. All rights reserved.
doi:10.1016/j.apsusc.2006.03.089

2. Experimental

Near-edge X-ray absorption fine structure spectroscopy measurements were conducted at the NIST/Dow soft X-ray material characterization facility, beamline U7A of the National Synchrotron Light Source at Brookhaven National Laboratory. In a NEXAFS experiment tunable soft X-rays are preferentially absorbed by the sample (characteristic depth of ≈200 nm) when the incident radiation is at the appropriate energy to allow the excitation of a core shell electron of a specific element (C, N, O or F) to a chemical bond specific unoccupied molecular orbital [10]. Due to the well-defined energy gap associated with a core shell to unoccupied orbital transition, NEXAFS is sensitive to the bonding characteristics of the element giving a discrete peak for each chemical bond. Auger electrons or fluorescence photons are emitted when the excited core hole from the irradiated sample relaxes. Auger electrons emitted from deep (>10 nm) within the film undergo multiple inelastic scattering and lose their kinetic energy within the film and hence cannot escape the surface potential to reach the detector. In contrast, electrons originating from near the top (1–6 nm for carbon K-edge electron yield spectra) of the film surface has sufficient kinetic energy to escape the surface potential. Electrons that escape the surface potential will have different final kinetic energies upon detection depending on their inelastic energy loss (depth of creation). By applying a negative voltage entrance grid bias (EGB) at the partial electron yield (PEY) detector, electrons of low kinetic energy can be rejected. As the negative entrance grid bias voltage is gradually increased, lower kinetic energy electrons are discriminated and the effective electron yield sampling depth gets closer to the film surface. This scheme uses EGB from −50 to −250 V probing the top 6–1 nm, respectively. The spectra were collected with the incident beam at the magic angle (54.7°) relative to the sample to remove any polarization dependence of the NEXAFS intensities. All PEY spectra in this paper were I_0 normalized for beam instabilities and monochromator absorption features using the total yield of clean gold I_0 mesh placed in the incident beam before the sample. The experimental standard uncertainty in the peak position is ±0.15 eV. The relative uncertainty in the NEXAFS intensity is less than ±2%.

Samples were prepared by spin coating solutions of methacrylate polymer with different PAGs onto silicon wafers of 2.54 cm diameter. The photoresist polymer is a proprietary formulation; however, for the purposes of these experiments the chemical details are not necessary. The two PAGs were triphenylsulfonium perfluorobutanesulfonate (TPS-PFBS) and triphenylsulfonium perfluorooctanesulfonate (TPS-PFOS) prepared at 5.0% and 6.7% by mass of photoresist in spin coating solvent. The nominal thickness was 220–240 nm as determined by optical reflectance methods. A photoresist film without PAG was also prepared as a control sample.

2.1. Theoretical considerations: depth profile

The integrated partial electron yield arising from the XY chemical bond observed by NEXAFS will be proportional to the total number density (ρ_{XY}) of those bonds. A constant similar to an extinction coefficient (A) will allow the Auger electron yield under constant incident flux conditions (I_0) of energy (E) to be determined. The precise yield will be subject to attenuation of Auger electrons from different depths and integration from the lower limit to upper limit in characteristic energy, $E_{\mathrm{XY}}^{\mathrm{L}}$ and $E_{\mathrm{XY}}^{\mathrm{U}}$, respectively. Therefore we should expect the following relation (1) to hold before considering the attenuation process:

$$I_{\mathrm{XY}} = A\rho_{\mathrm{XY}} I_0 = \int \mathrm{d}z \int_{E_{\mathrm{XY}}^{\mathrm{L}}}^{E_{\mathrm{XY}}^{\mathrm{U}}} I(E,z)\,\mathrm{d}E \tag{1}$$

Under depth-independent illumination, the soft X-rays are absorbed at a distance z from the surface leading to the Auger electrons emission as shown in Fig. 1. This electron yield cascade will subsequently be attenuated through the inelastic scattering over the distance z yielding a differential electron yield $\mathrm{d}I_{\mathrm{XY}}^{0} = A\rho_{\mathrm{XY}}(z) I_0\,\mathrm{d}z$. The superscript '0' denotes an ideal electron yield that has not been attenuated by the medium. The attenuation process will generally be written as, $I_{\mathrm{XY}} = I_{\mathrm{XY}}^{0}(z)\,\mathrm{e}^{-z/\lambda^*}$, where λ^* is the electron mean-free path. Following the work of Genzer et al. the probed mean-free path (or effective sampling depth) can be tuned by varying the entrance grid bias [11] of the partial electron yield detector. The entrance grid-dependent mean-free path, $\lambda^*[\mathrm{EGB}] = 1.04(3.667 + 0.009\mathrm{EGB})$ determined in that work is used here to quantify the depth profile. The inset of Fig. 1 shows the schematic of the attenuation process in which the detected Auger electron yield drops in an exponential manner with tuned mean-free path (or effective sampling depth) as a function of EGB. The characteristic depth is given by e^{-1}. Therefore, by combining the electron yield with the attenua-

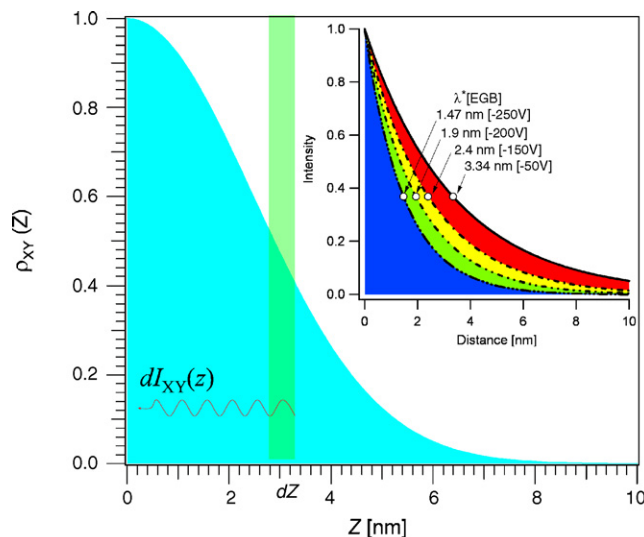

Fig. 1. Schematic of the NEXAFS depth profile of a model concentration profile of the X–Y bond. The highlighted element of thickness dz at a depth z absorbs soft X-ray of a given energy leading to an electron yield of dI_{XY}, that is subject kinetic energy loss upon traversing the distance z, characterized by the mean-free path. Inset: depth profiling as a function of entrance grid bias. The measured electron yield is controlled by the different bias, equivalently mean-free path.

Table 1
Model profiles

	Bond-sensitive EGB NEXAFS
Gaussian profile	$AI_0\rho_0\sqrt{\frac{\pi}{2}\sigma^2}\,\mathrm{e}^{-\sigma^2/2\lambda^*[\mathrm{EGB}]^2}\,\mathrm{Erfc}\left(\frac{\sigma}{\sqrt{2}\lambda^*[\mathrm{EGB}]}\right)$
Constant density	$AI_0\rho_0\lambda^*[\mathrm{EGB}]$
Finite surface layer	$AI_0\rho_0\lambda^*[\mathrm{EGB}](1-\mathrm{e}^{-d/\lambda^*[\mathrm{EGB}]})$

$\lambda^*[\mathrm{EGB}] = 1.04(3.667 + 0.009\mathrm{EGB})$ taken from Genzer et al. [11].

tion, the predicted partial electron yield as a function of $\lambda^*[\mathrm{EGB}]$ for bond XY is:

$$I_{\mathrm{XY}} = AI_0\int_0^{\infty} \mathrm{d}z\,\rho_{\mathrm{XY}}(z)\,\mathrm{e}^{-z/\lambda^*[\mathrm{EGB}]} \tag{2}$$

A model profile ($\rho_{\mathrm{XY}}(z)$) can be substituted allowing a comparison between experiment and theory. The results for three cases are provided: (1) constant concentration of the material associated with bond XY; (2) surface layer of finite thickness and (3) a Gaussian profile as shown in Table 1.

3. Results and discussions

The utility of NEXAFS for understanding photoresist chemistry, reaction and segregation was previously analyzed by a principal component analysis [12,13]. This involves scaling the spectra of the pure components to that of the mixture. However, an approach to quantify the surface depth profile was not examined. Here, a model system is applied in which the analyte (absorber) is spectrally distinct from the polymer matrix by the presence of aromatic groups on the PAG as shown in Scheme 1.

Fig. 2 shows the NEXAFS carbon K-edge spectra for the pure methacrylate photoresist (dotted line) and photoresist containing TPS-PFOS (solid lines). The incident photon energy is scanned from 280 to 330 eV and the electron yield is measured at the detector as a function of the entrance grid bias from −250 V (immediate surface) to −50 V (top several nm). All the C-Auger electrons are rejected from the detector at −320 V which is shown by the detector null response. The spectral intensity is highest at the smallest bias (−50 V) due to the greater number of electrons admitted to the detector from the larger sampling depth (inset of Fig. 1); the intensity is progressively reduced as the bias is increased to −250 V in −50 V decrements. The sharp peak at 285 eV is the C $1s\rightarrow\pi^*_{\mathrm{C=C}}$ transition arising from the triphenyl groups on the PAG as shown in the inset of Fig. 2. The sharp peak at 288.5 eV is the $1s\rightarrow\pi^*_{\mathrm{C=O}}$ arising from the methacrylate photoresist. All NEXAFS spectra are pre-edge (below 280 eV) subtracted to zero for baseline normalization. The post-edge (around 325–330 eV) jump intensity is proportional to the total carbon content, since at these energies all the C 1s electrons are excited to the continuum. The C–F bond from the PAG is not distinct in these spectra, but typically appears at 295.1 eV C $1s\rightarrow\sigma^*_{\mathrm{C-F}}$. The inset to Fig. 2 highlights the C $1s\rightarrow\pi^*_{\mathrm{C=C}}$, region of interest for the profiling. The neat polymer without PAG has a bias-independent background as seen by the dotted lines, but the resist/PAG mixture has strong bias dependence. The integrated peak intensity is directly proportional to the C=C molar bond (number) density allowing a quantification of the PAG composition as a function of depth without interference of the photoresist chemistry. These photoresists are fully saturated and hence do not contribute to C $1s\rightarrow\pi^*_{\mathrm{C=C}}$ NEXAFS intensity. The saturation of the photoresist polymer provides high transparency at the photolithographic printing wavelength of 193 nm, which is absorbed strongly by aromatic groups.

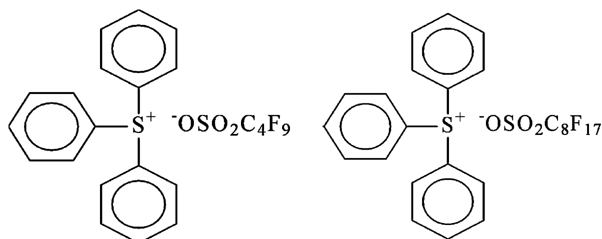

Scheme 1. Triphenylsulfonium perfluorobutanesulfonate (left) and perfluorooctanesulfonate (right) photoacid generators.

3.1. Photoacid generator depth profile

The NEXAFS data of Fig. 2 were integrated about the peak center at 285 eV with a Gaussian function providing the integrated electron yield intensity ($I^{\mathrm{EY}}_{\mathrm{C=C}}$) as a function of entrance grid bias. The model approach, described earlier, is followed by plotting $I^{\mathrm{EY}}_{\mathrm{C=C}}$ versus EGB as shown in Fig. 3 (left) for the TPS-PFOS system. As the applied EGB becomes more negative, we expect the total electron yield to decrease, which is

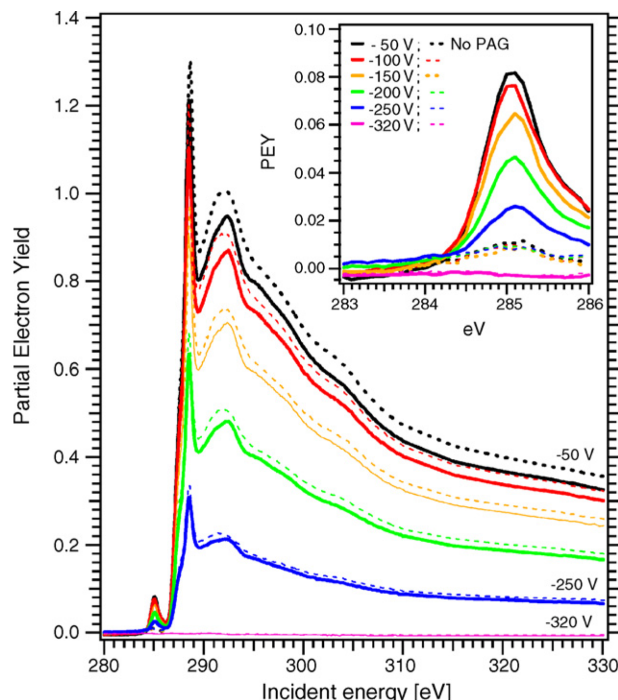

Fig. 2. NEXAFS spectra of the pure photoresist (dotted lines) and resist containing 6.7% by mass TPS-PFOS photoacid generator (solid lines) as a function of entrance-grid bias from −50 to −250 V. At −320 V, no signal is detected. The inset highlights the $\pi^*_{\mathrm{C=C}}$ region which allows direct quantification of the triphenyl groups of the photoacid generator.

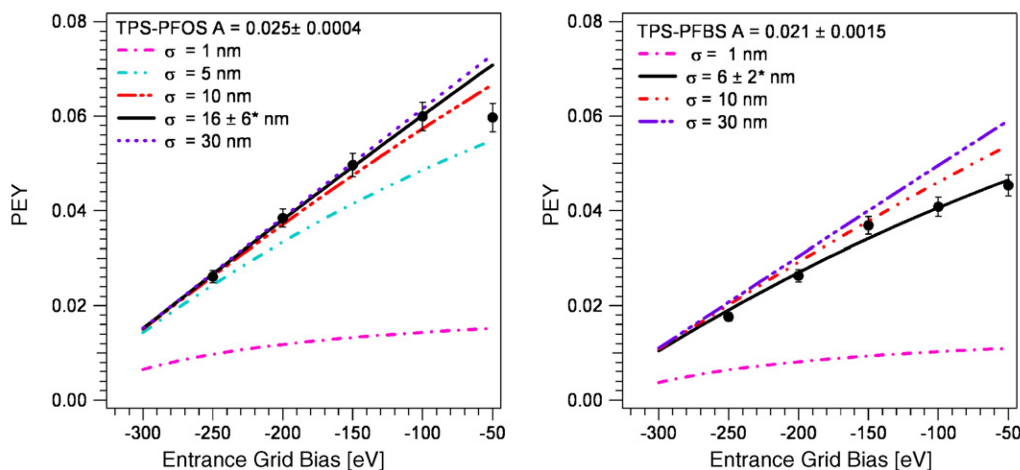

Fig. 3. Plot of the integrated partial electron yield (PEY) between 283 and 285.5 eV vs. entrance grid bias for the TPS-PFOS (left) and TPS-PFBS systems (right). The solid lines are regression results to the Gaussian profile model with decay length indicated by the '*'. The characteristic decay length for the TPS-PFOS is 16 ± 6 nm, while the TPS-PFBS quantified by a 6 ± 2 nm surface decay length to the bulk. The sensitivity of the model to the Gaussian width parameter is shown by the dotted lines.

observed experimentally. While the Gaussian theoretical compositional profile (refer to Table 1) lacks atomic-level detail, it is convenient to understand the compositional profile, providing a general approach to quantify the experimental data. Before applying the model to the experimental data, a background was determined by fitting the small bias (−320 V)-independent intensity of the pure resist, which is then subtracted from the resist/PAG mixture. The solid circles are the data with 5% error bars. The TPS-PFOS system is fit to the two-parameter equation using a non-linear least squares method to extract the prefactor ($AI_0\rho_0$) and the characteristic decay length for the surface density profile, σ. The curve indicated by the '*' is the value obtained by non-linear least squares regression to the Gaussian profile model. This concludes the surface is enriched with the TPS-PFOS with a characteristic length scale of 16 ± 6 nm. While such a large length scale can be measured by the EGB approach, it is highly sensitive to σ. We illustrate this by fixing the concentration prefactor and illustrate the sensitivity of the partial electron yield with EGB under varied σ from 1 to 30 nm, which clearly do not match the experimental data. The family of profiles cannot be distinguished experimentally between 16 and 30 nm. Therefore the bias experiment suggests the TPS-PFOS, while surface enriched, extends deep within the film. The enrichment above the bulk level of an iodonium PFOS PAG was observed by Lenhart et al. [1] and was found to increase the rate of acid catalyzed reaction at the near-film surface compared to the bulk.

In contrast, the TPS-PFBS system shown in Fig. 3 (right) depicts a clear curvature in the experimental data that is fit using the Gaussian profile model leading to a measurable surface composition with decay of width 6 ± 2 nm. Since our approach highlights the profile character, the true bulk concentration of the 220 nm thick film cannot be measured by the partial electron yield approach. In this case, we conclude that the TPS-PFBS system exhibits a slight compositional heterogeneity at the surface with a small characteristic length of 6 nm. The data are not consistent with a surface layer of width 10 nm as shown by comparing the model with varied values of σ. The profile behavior is distinct from the TPS-PFOS case. Fig. 4 summarizes our observations by plotting the Gaussian profile model with the experimentally determined parameters. The ordinate highlights the proportionality to molar concentration and it is clear that the TPS-PFOS has a higher surface concentration than the TPS-PFBS, even though they are prepared at the same molar concentrations. It would be interesting to examine how these profiles are modified by photoresist processing conditions, film thickness, or water immersion. Since immersion lithography is in development the direct quantification of PAG concentration, on wafer, must be understood.

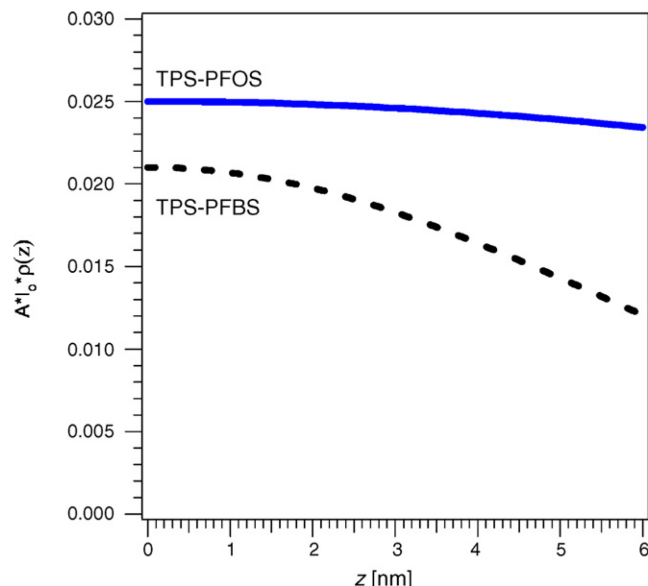

Fig. 4. Results from the depth profile study by substituting the Gaussian width and prefactor parameters into the model profile. Within the depth resolution of the NEXAFS technique the TPS-PFOS is extensively segregated with a characteristic depth of 16 nm, whereas the TPS-PFBS does exhibit an excess with decay length of 6 nm.

4. Conclusions

A method for depth profiling the chemistry of thin polymer films was presented with an example of the surface segregation of PAGs, critical components in photoresist materials. A varying entrance grid bias methodology distinguishes a slight surface excess for a triphenylsulfonium perfluorobutanesulfonate with profile of characteristic length 6 nm. A triphenylsulfonium perfluorooctanesulfonate PAG, however, has a thick surface layer of 16 nm, suggesting this PAG is present with characteristic length scales larger than accessible by the partial electron yield depth profiling approach. The NEXAFS technique provides a high resolution measurement in which small chemical bond differences can be highlighted. This approach can be used to understand the influence of water immersion on PAG leaching and depth profiling.

References

[1] J.L. Lenhart, D.A. Fischer, S. Sambasivan, E.K. Lin, R.L. Jones, C.L. Soles, et al. Langmuir 21 (9) (2005) 4007–4015.

[2] R.R. Dammel, F.M. Houlihan, R. Sakamuri, D. Rentkiewicz, A. Romano, J. Photopolym. Sci. Technol. 17 (4) (2004) 587–601.

[3] M. Rothschild, T.M. Bloomstein, R.R. Kunz, V. Liberman, M. Switkes, S.T. Palmacci, et al. J. Vac. Sci. Technol. B 22 (6) (2004) 2877–2881.

[4] W.D. Hinsberg, et al. in: Proceedings of the SPIE Advances in Resist Technology and Processing XXI 5376, 2004, p. 21.

[5] J.C. Taylor, R.J. Lesuer, C.R. Chambers, F.R.F. Fan, A.J. Bard, W.E. Conley, et al. Chem. Mater. 17 (16) (2005) 4194–4203.

[6] R.D. Allen, P.J. Brock, L. Sundberg, C.E. Larson, G.M. Wallraff, W.D. Hinsberg, et al. J. Photopolym. Sci. Technol. 18 (5) (2005) 615–619.

[7] K.E. Uhrich, E. Reichmanis, F.A. Baiocchi, Chem. Mater. 6 (3) (1994) 295–301.

[8] N. Sundararajan, C. Keimel, N. Bhargava, C. Ober, J. Opitz, R.D. Allen, et al. J. Photopolym. Sci. Technol. 12 (3) (1999) 457–468.

[9] H. Krautter, F. Houlihan, R. Hutton, I. Rushkin, R. Opila, in: Proceedings of the SPIE Advances in Resist Technology and Processing XVII 3999, 2000, pp. 1070–1078.

[10] J. Stöhr, NEXAFS Spectroscopy, Springer-Verlag, New York, 1992.

[11] J. Genzer, E.J. Kramer, D.A. Fischer, J. Appl. Phys. 92 (12) (2002) 7070–7079.

[12] J.L. Lenhart, R.L. Jones, E.K. Lin, C.L. Soles, W.L. Wu, D.A. Fischer, et al. J. Vac. Sci. Technol. B 20 (6) (2002) 2920–2926.

[13] E.L. Jablonski, V.M. Prabhu, S. Sambasivan, E.K. Lin, D.A. Fischer, D.L. Goldfarb, et al. J. Vac. Sci. Technol. B 21 (6) (2003) 3162–3165.